Fabrication of Segmented Cavity Films and Their Application to Nanocomposite Materials

Hirohmi Watanabe and Toyoki Kunitake*

Spatio-Temporal Function Materials Research Group, Frontier Research System (FRS), The Institute of Physical and Chemical Research (RIKEN), Hirosawa 2-1, Wako-shi, Saitama 351-0198, Japan

Received January 27, 2005. Revised Manuscript Received April 21, 2005

The fabrication of a novel organic−inorganic nanocomposite film in which functional molecules are incorporated with 2-dimensional (2-D) selectivity is described. The 2-D selectivity is attained by photofabrication of segmented nanocavities which can accommodate organic molecules. A composite thin film of 4-azidobenzoic acid (ABA) and titania (TiO_2) was obtained by the surface sol−gel process of their mixed precursors. UV irradiation of the ABA/TiO_2 film caused decomposition (N_2 gas evolution) of the azide group of ABA, and nanocavities were created within the matrix. The nanocavity can accommodate ABA and sulforhodamine B molecules. 2-D sequential incorporation of these molecules into different film segments was made possible by formation of segmented nanocavities via photodecomposition of ABA through a photomask. The current approach allows incorporation of varied functional molecules into segmented nanocavities. Designed 2-D arrangement of the nanocavity within thin film matrixes would find many novel applications.

Introduction

Molecular-precision composite materials (organic−inorganic and inorganic−inorganic nanocomposite materials) have been recognized as one of the most promising topics in materials research.[1] These materials are produced by widely varied methodologies such as the conventional sol−gel process,[2−5] self-assembly procedures,[6−8] and assembly of nano building blocks (ANBB).[9−11] Practically useful systems such as photoswitches,[12,13] nonlinear optics (NLO),[14] pH sensors,[15] electroluminescent diodes,[16] and catalysts[17,18] have been created by using these materials. Many functional improvements are anticipated, if spatial arrangements of the functional unit can be precisely designed in these materials. Layer-by-layer separation of molecular layers is a convenient way to achieve the controlled arrangement in the *z*-dimension. However, the layer-by-layer deposition cannot give 2-D designed (or patterned) structures within the layer plane. Lithographic surface imaging by using a functionalized self-assembled monolayer (SAM) is one of the appropriate methods to achieve the controlled arrangement within the layer plane.[19−22] However, this method is restricted to control of the nanocomposition on the surface of the SAM. It is strongly desired to develop a means to achieve 2-D design within the ultrathin matrix.

In our previous work, we demonstrated molecular imprinting effects for titania and other metal oxide films which were fabricated by the surface sol−gel process. Selective rebinding of organic template molecules was observed after template removal. Functional selectivity, structure selectivity, regioselectivity, and stereoselectivity were observed in such rebinding experiments.[23] In the case of similar composite films of dendrimers and poly(acrylic acid), low-pressure oxygen plasma treatment created the corresponding regular and irregular nanocavities within the matrix.[24,25] Removal of incorporated metal ion by alkaline treatment was also

* To whom correspondence should be addressed. E-mail: kunitake@ruby.ocn.ne.jp.

(1) Schmidt, H.; Kaiser, A.; Patzelt, H.; Scholze, H. *J. Phys., Colloq.* **1982**, *C9*, 275.
(2) Sanchez, C.; Ribot, F. *New J. Chem.* **1994**, *18*, 1007.
(3) Avnir, D.; Kaufman, V. R.; Reisfeld, R. *J. Non-Cryst. Solids* **1985**, *74*, 395.
(4) Landry, C. J. T.; Coltrain, B. K.; Wesson, J. A.; Zumbulyadis, N.; Lippert, J. L. *Polymer* **1992**, *33*, 1496.
(5) Morikawa, A.; Iyoku, Y.; Kakimoto, M.; Imai, Y. *J. Mater. Chem.* **1992**, *2*, 679.
(6) Stein, A.; Melde, B. J.; Schroden, R. C. *Adv. Mater.* **2000**, *12*, 1403.
(7) Lim, M. H.; Stein, A. *Chem. Mater.* **1999**, *11*, 3285.
(8) Soler-Illia, G. J. de A. A.; Rozes, L.; Boggiano, M. K.; Sanchez, C.; Turrin, C.-O.; Caminade, A.-M.; Majoral, J.-P. *Angew. Chem., Int. Ed.* **2000**, *39*, 4250.
(9) Sanchez, C.; Soler-Illia, G. J. de A. A.; Ribot, F.; Lalot, T.; Mayer, C. R.; Cabuil, V. *Chem. Mater.* **2001**, *13*, 3061.
(10) Hoebbel, D.; Endres, K.; Reinert, T.; Pitsch, I. *J. Non-Cryst. Solids* **1994**, *176*, 179.
(11) Banse, F.; Ribot, F.; Tolédano, P.; Maquet, J.; Sanchez, C. *Inorg. Chem.* **1995**, *34*, 6371.
(12) Schaudel, B.; Guermeur, C.; Sanchez, C.; Nakatani, K.; Delaire, J. *J. Mater. Chem.* **1997**, *7*, 61.
(13) Sasaki, K.; Nagamura, T. *Appl. Phys. Lett.* **1997**, *71*, 434.
(14) Lebeau, B.; Brasselet, S.; Zyss, J.; Sanchez, C. *Chem. Mater.* **1997**, *9*, 1012.
(15) Rottman, C.; Grader, G.; De Hazan, Y.; Melchior, S.; Avnir, D. *J. Am. Chem. Soc.* **1999**, *121*, 8533.
(16) Dantas de Moras, T.; Chaput, F.; Lahlil, K.; Boilot, J.-P. *Adv. Mater.* **1999**, *11*, 107.
(17) Shangguan, W.; Yoshida, A. *J. Phys. Chem. B* **2002**, *106*, 12227.
(18) Machida, M.; Nagasaki, S.; Kijima, T. *Stud. Surf. Sci. Catal.* **2002**, *143*, 863.
(19) Dressick, W. J.; Calvert, J. M. *Jpn. J. Appl. Phys.* **1993**, *32*, 5829.
(20) Ingall, M. D. K.; Honeyman, C. H.; Mercure, J. V.; Bianconi, P. A.; Kunz, R. R. *J. Am. Chem. Soc.* **1999**, *121*, 3607.
(21) Aizenberg, J.; Black, A. J.; Whitesides, G. M. *Nature* **1999**, *398*, 495.
(22) Han, S. W.; Lee, I.; Kim, K. *Langmuir* **2002**, *18*, 182.
(23) Lee, S.-W.; Ichinose, I.; Kunitake, T. *Langmuir* **1998**, *14*, 2857.
(24) Huang, J.; Ichinose, I.; Kunitake, T.; Nakao, A. *Langmuir* **2002**, *18*, 9048.
(25) Huang, J.; Ichinose, I.; Kunitake, T. *Chem. Commun.* **2002**, 2070.

10.1021/cm050191a CCC: $30.25
Published on Web 06/08/2005

Scheme 1. A Schematic Figure of the Preparation of a 2-D Arranged Nanocomposite Material[a]

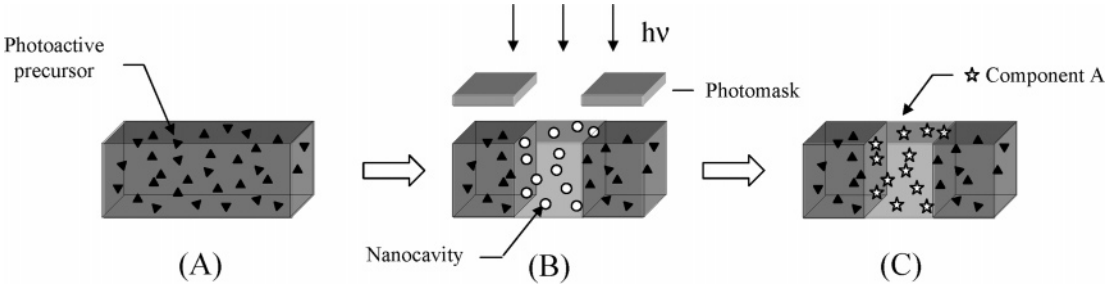

[a] Key: (a) surface sol−gel preparation of a photoactive precursor-incorporated TiO_2 thin film; (b) fabrication of a segmented nanocavity film by photopatterning; (c) accommodation of the segmented nanocavity with a small molecule.

useful to create nanocavities.[26−28] However, positionally specified arrangements of the nanocavity could not be achieved by these methods. In the present study, we propose a novel, unique approach for the fabrication of segmented nanocomposite materials. This approach is based on photofabrication of segmented nanocavities, followed by doping the nanocavity with other molecules (Scheme 1). Photoactive agents play a crucial role in the fabrication of segmented nanocavities. They cause generation of gases (N_2, CO_2, O_2, etc.) upon photoirradiation to produce nanocavities within the matrix (Scheme 1B). An undeniable advantage of the photochemical process is the geometrically selective modification by the use of photomasks and the laser imaging system. These lead to designed 2-dimensional (2-D) arrangements of nanocavities. The segmented nanocavities can accommodate other organic and inorganic compounds such as fluorescence dyes and metal ions, giving 2-D designed molecular-precision composite materials (Scheme 1C).

Experimental Section

Chemicals. 4-Azidobenzoic acid (abbreviated as ABA) was obtained from Tokyo Kasei and used without further purification. Titanium *n*-butoxide (abbreviated as Ti(O-*n*-Bu)$_4$) was obtained from Gelest. Sulforhodamine B (dye content <75%) was obtained from Aldrich. All of the solvents in this study were purchased from Kanto Chemicals and used without further purification. Spectroscopic grade acetonitrile was used for the spectroscopic measurements.

Preparation of $TiO_4O_4(OH)_4$(O-*n*-Bu)$_4$(ABA) Sol. Ti(O-*n*-Bu)$_4$ (100 mM) was dissolved in a 2:1 (v/v) mixture of toluene and ethanol. ABA (25 or 50 mM) was added to the solution, and the mixture was stirred at room temperature for 24 h. A small amount of water was then added to the solution, and the mixture was stirred for more than 1 h. The complete reaction of Ti(O-*n*-Bu)$_4$, ABA, and H_2O will produce $TiO_4O_4(OH)_4$(O-*n*-Bu)$_4$(ABA), as reported in our previous work.[19] The mixture was diluted 20 times by toluene and used as a dipping solution.

Surface Sol−Gel Process. Chemical modification of the substrates prior to deposition is essential for the reproducible formation of surface sol−gel thin films. Gold and quartz substrates were immersed into 3 wt % 2-mercaptoethanol in ethanolic solution and 1 wt % ethanolic KOH (ethanol:water = 3:2), respectively. After the immersion for a few minutes, these substrates were rinsed with ethanol and dried by flushing with N_2 gas. Gold substrates and gold-coated quartz crystal microbalance (QCM) resonators were employed for IR and QCM measurements, respectively. Quartz substrates were employed for UV and fluorescence measurements.

The surface of these substrates became hydrophilic after the chemical modification, and the surface sol−gel process was performed on the hydroxylated surface. These substrates were immersed into the dipping solution for 1 min. Subsequently, the substrate was soaked in toluene and sonicated for 1 min to remove physically adsorbed species. After N_2 gas was flushed for 1 min, the substrate was kept in air for 3 min to complete the hydrolysis reaction of $TiO_4O_4(OH)_4$(O-*n*-Bu)$_4$(ABA). Twenty cycles of the surface sol−gel process were repeated.

Measurements. UV−vis absorption spectra and fluorescence spectra were obtained by a Shimadzu UV-3100PC UV−vis scanning spectrophotometer and a Jasco FP-6500 fluorescence spectrophotometer, respectively. QCM measurements were conducted using 9 MHz QCM gold electrodes (USI system, Fukuoka). Attenuated total reflection FT-IR spectra were obtained by a Thermo Nicolet Nexus 670 FT-IR spectrometer using gold-coated microslides as substrate. UV irradiation was performed by using a low-pressure mercury lamp (UVB-X, Sen Light Corp.) without any filter. Fluorescence microscopic observation was carried out on an Olympus BX60 fluorescence microscope.

Results and Discussion

Preparation of an ABA/TiO_2 Film. A graphic representation of layer-by-layer growth of an ABA-incorporated TiO_2 film (ABA/TiO_2) is shown in Scheme 2. First, $TiO_4O_4(OH)_4$-(O-*n*-Bu)$_4$(ABA) sol is chemisorbed on the surface of a hydroxylated substrate by immersion. Removal of physically adsorbed components and subsequent hydrolysis give metal oxide ultrathin layers with molecular thickness. By repetition of this process (chemsorption, rinsing, and drying), ABA/TiO_2 multilayer films are formed with an incremental thickness increase.

QCM and UV absorption measurements are useful for monitoring the layer-by-layer growth. Figure 1 shows QCM frequency changes of the ABA/TiO_2 film as recorded after each cycle of the surface sol−gel process. The QCM frequency decreased linearly with an increase of the number of layering steps. When the concentration of ABA was 25 mM, the frequency decrease was reproducible for 20 cycles with a 145 ± 30 Hz shift for one cycle. In the case of 50 mM ABA, the frequency shift was 36 ± 8 Hz for one cycle. The smaller adsorbed mass at the high concentration of ABA may be due to the decrease of the ratio of the hydroxylated

(26) He, J.; Ichinose, I.; Kunitake, T.; Nakao, A. *Langmuir* **2002**, *18*, 10005.
(27) He, J.; Ichinose, I.; Fujikawa, S.; Kunitake, T.; Nakao, A. *Chem. Mater.* **2002**, *14*, 3493.
(28) He, J.; Fujikawa, S.; Kunitake, T.; Nakao, A. *Chem. Mater.* **2003**, *15*, 3308.

Scheme 2. Schematic Figure of the Layer-by-Layer Growth of a Thin Film by the Surface Sol−Gel Process

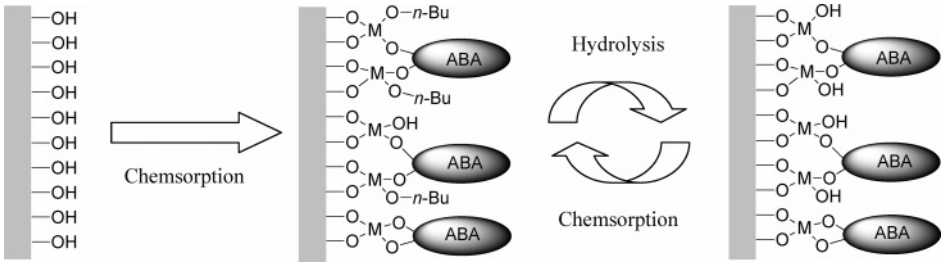

surface. A certain fraction of the layer surface may be covered by ABA, and these areas are inactive toward layer-by-layer growth. Slower hydrolysis of the titanium alkoxide at the high fraction of the organic molecule can also cause smaller adsorbed mass.[19] In the subsequent deposition, the ABA concentration of the dipping solution was fixed at 25 mM.

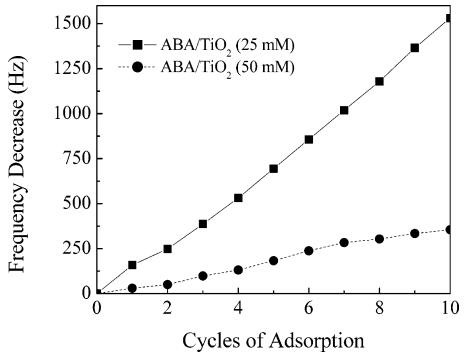

Figure 1. QCM frequency changes of an ABA-incorporated TiO_2 film (ABA/TiO_2) at individual cycles of the surface sol−gel process.

Figure 2 shows the UV absorption spectrum of the ABA/TiO_2 film at each cycle of the surface sol−gel process. ABA/TiO_2 films show a characteristic absorption at 270 nm due to the azide group of ABA (λ_{max} = 268 nm in acetonitrile). This absorption linearly increased with an increase of the number of preparation steps as indicated in the inset of Figure 2. It is clear that an ABA molecule was incorporated into the TiO_2 matrix in a regular manner.

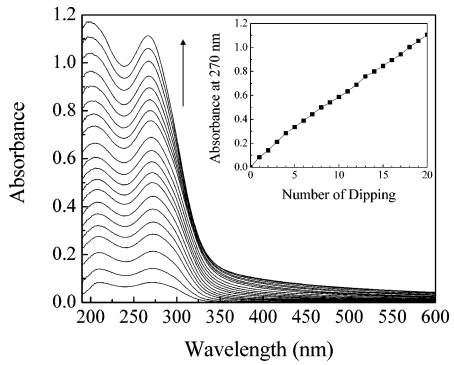

Figure 2. UV absorption spectra of the ABA/TiO_2 film at each cycle of the surface sol−gel process. The inset shows the absorption at 270 nm at each preparation step.

Fabrication of Nanocavity Films. Attenuated total reflection IR spectra of the ABA/TiO_2 films before and after UV irradiation are shown in Figure 3A. The ABA/TiO_2 film showed a strong absorption peak around 2125 cm^{-1} before UV irradiation which originates from the asymmetric stretching vibration of the azide group ($-N_3$) of ABA. Small absorption peaks at around 1650 and 2000−1700 cm^{-1} were assigned as a stretching vibration of the carbonyl group (C═O) and a characteristic absorption of the *para*-substituted

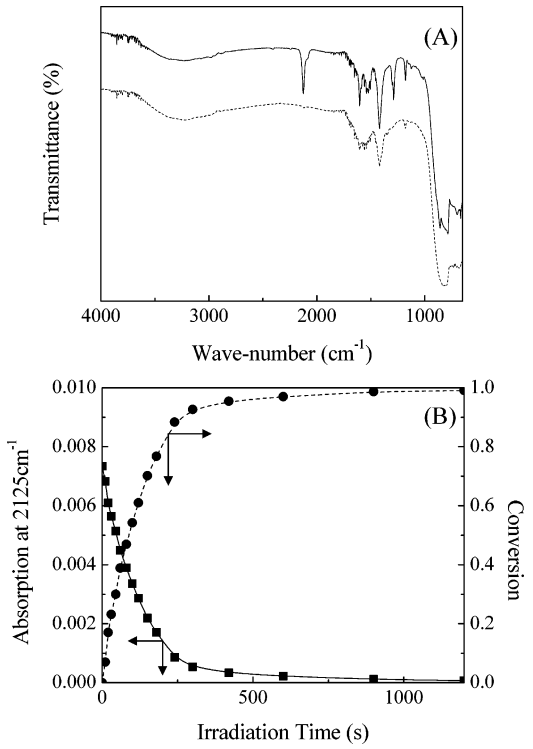

Figure 3. (A) Refraction IR spectroscopy of the ABA/TiO_2 film before (solid line) and after (dashed line) the irradiation of 254 nm UV light for 240 s. (B) Absorption at 2125 cm^{-1} (left axis) and the conversion of the azide groups (right axis) during UV irradiation.

benzene ring of ABA, respectively. The absorption of the azide group disappeared completely after UV irradiation for 240 s, although other peaks remained intact. Clearly, the loss of the azide group is the major photochemical reaction upon UV irradiation. Structural determination of the photoproduct by NMR and IR spectroscopies was not definite because of the complex nature of the final photoproducts that is common to the chemical reaction of photogenerated active nitrene (Scheme 3).[29] Figure 3B is the time course of the IR spectral intensity of the azide groups (at 2125 cm^{-1}) and the total conversion during UV irradiation. The IR intensity of the azide group underwent a very rapid decrease during UV irradiation. According to the conversion data, it is clear that

(29) Turro, N. J. In *Modern Molecular Photochemistry*; University Science Books: Sausalito, CA, 1976; pp 550−557.

Scheme 3. Photoelimination of Nitrogen from the Azide Compound and the Subsequent Chemical Reaction of Nitrene

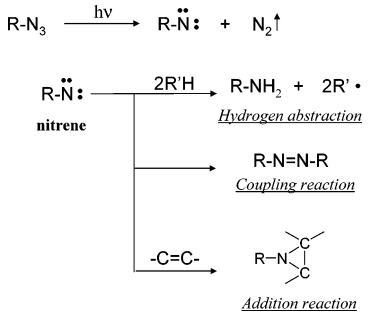

the decomposition of the azide groups proceeds to over 90% completion within the 240 s irradiation. The corresponding UV absorption spectra (ABA/TiO_2 (20 layers), on quartz) during UV irradiation are shown in Figure 4. An absorption decrease at around 200 and 270 nm and an increase at 230−260 and 330−430 nm were observed with well-defined isosbestic points at 225, 252, and 331 nm up to irradiation for 240 s. These adsorption spectral changes are similar to that observed for ABA in acetonitrile, demonstrating that similar photochemical reactions proceed in solution and within the metal oxide matrix. The presence of the isosbestic points suggests that ABA undergoes one-step photoreaction without any competitive reactions up to 240 s. However, longer irradiation beyond 240 s causes further photodegradation of the primary photoproduct. As a result, isosbestic points were lost as shown in Figure 4. After irradiation for 2400 s, the shape of the absorption spectrum was quite similar to that of TiO_2 films which were obtained by the surface sol−gel process. This result suggests that prolonged irradiation caused photocalcination of ABA molecules. Incidentally, no significant change in the UV spectrum was observed for pure TiO_2 films except for a slight decrement at around 190−220 nm due to the photodegradation of unreacted alkyl butoxide.

The photodecomposition process can be pursued by QCM measurement. Normalized mass changes of the ABA/TiO_2 and TiO_2 films during UV irradiation are shown in Figure 5. The ABA/TiO_2 film showed a large mass decrease by UV irradiation (2.23% loss against the total mass of the ABA/TiO_2 film), while only a slight change was observed for the TiO_2 film. The mass of total ABA molecules within the ABA/TiO_2 film is estimated to be 12.8% from comparisons of QCM frequency changes before and after chemical

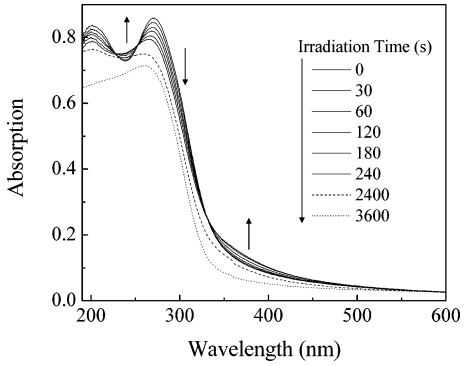

Figure 4. Absorption spectra of the ABA/TiO_2 film during UV irradiation.

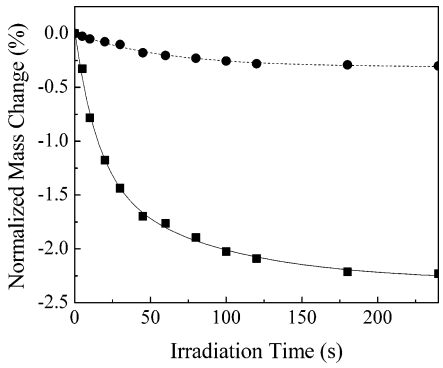

Figure 5. Normalized mass changes of the ABA/TiO_2 (squares) and TiO_2 (circles) films during UV irradiation.

removal of the incorporated ABA molecule by soaking in 1% ammonia solution. And the mass of the N_2 moiety is calculated as 2.21% by using the molecular weights of ABA (MW = 163.04) and N_2 (MW = 28.01) (=12.8/163.04 × 28.01). It is clear that the observed weight loss (2.23%) by UV irradiation is almost identical as that of the calculated total mass of two nitrogen atoms of ABA in the ABA/TiO_2 film. This result also suggests that only the loss of N_2 from the azide groups of ABA occurred during the initial stage of photoirradiation.

Direct observation of the individual nanocavity by transmission electron microscopy was attempted for the ABA/TiO_2 layer on a silicon oxide-coated TEM grid. However, no difference was observed before and after UV irradiation. Subsequently, atomic force microscopy was employed to compare the surface morphology of the ABA/TiO_2 film before and after UV irradiation. The surface roughness and height profile were essentially identical (within 2 nm) between the two. It is clear that the photodecomposition of ABA did not cause any change in the surface morphology. Therefore, the nanocavities must be created within the TiO_2 matrix.

Readsorption Step. Subsequently, accommodation of the nanocavity was examined by using the ABA molecule as a refill agent. ABA was again used to simplify the argument. An ABA/TiO_2 film that had been subjected to UV irradiation for 240 s was immersed in 5 mM ABA in acetonitrile for given periods of time, rinsed with pure acetonitrile, and air-dried. Mass changes during the readsorption were monitored by the QCM frequency and normalized relative to the total mass of the irradiated film. At this experimental condition, residues of the photodecomposed ABA molecule still exist in the matrix.

It is desirable to examine the accommodation capability of the nanocavity after complete removal of the photoproduct. In fact, residues of the photoreaction can be removed completely by washing the film with polar solvents. However, this treatment removes unreacted ABA molecules simultaneously. This situation is not desirable in the following patterning process where irradiated and nonirradiated regions should be differentiated. Complete photodegradation of the residues by prolonged irradiation produces morphology changes of the film. Therefore, we chose the experimental conditions in which photochemical residues still remained in the matrix.

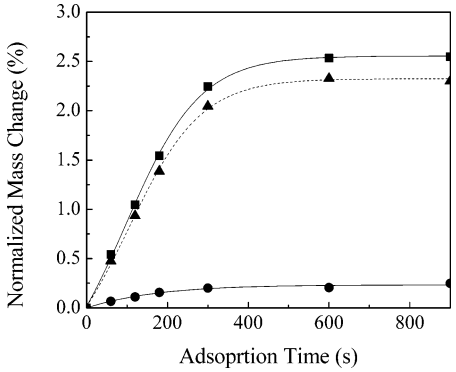

Figure 6. Normalized mass changes of irradiated ABA/TiO_2 (squares) and nonirradiated ABA/TiO_2 (circles) films during the readsorption step. The amount of interior ABA molecules is calculated as depicted by the dashed line.

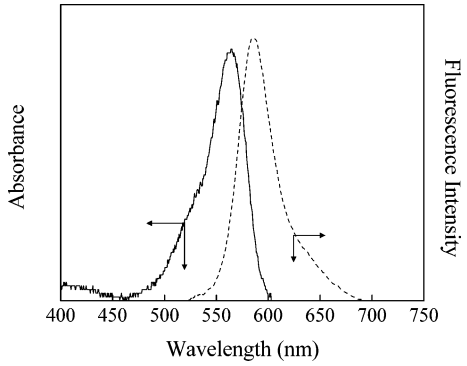

Figure 7. Absorption and fluorescence spectra of a sulforhodamine B-doped TiO_2 film.

As shown in Figure 6, the normalized mass of the nanocavity film (irradiated ABA/TiO_2 film) was remarkably enhanced with an increase in the immersion time and reached saturation at around 600 s. In contrast, only a slight mass increase was observed in the no-cavity film (nonirradiated ABA/TiO_2 film). Since the increase probably came from the chemically adsorbed ABA molecules on the surface (physically adsorbed mass is removed completely by rinsing), it was subtracted from mass increase of the cavity film. Fortunately, the subtraction does not affect significantly the mass increase of the cavity film as shown in Figure 6.

The amount of readsorbed ABA molecules was calculated from QCM frequency changes. It was assumed in this calculation that all of the photoproducts of ABA remained within the matrix as 4-aminobenzoic acid even during the readsorption procedure. The total amount of the readsorbed ABA was estimated to be 19.5% of the original amount of ABA, and this is composed of 1.9% surface adsorption and 17.6% inner accommodation (see the Supporting Information). It is clear that the ABA molecule can be accommodated in the cavity even in the presence of the photoproducts. IR measurement also confirmed the incorporation of ABA into the nanocavity. The absorption peak of the azide group at 2125 cm^{-1} appeared again, and the amount was estimated to be 20% of the original amount of ABA. We have also examined readsorption for the sample in which the nanocavities were created by chemical removal of the template ABA molecule through treatment with 1% ammonia solution. It was surprising that the amount of the incorporated ABA molecules was comparable to that of the photochemically fabricated nanocavity film. This suggests that the size of the photofabricated nanocavities is similar to that of the nanocavities (molecular dimension) formed by chemical template removal.

Fabrication of a Patterned Ultrathin TiO_2 Film. From the above result, it is clear that the fabricated nanocavity can accommodate small molecules. Incorporation of other small organic compounds into the nanocavity will lead to fabrication of molecular-precision composite films. We chose for this purpose sulforhodamine B as fluorescence proves to confirm the doping within the nanocavity. A photoirradiated ABA/TiO_2 film (240 s of irradiation) was immersed in a 5 mM solution of sulforhodamine B in acetonitrile for 600 s and rinsed with acetonitrile to remove the physically adsorbed molecules. Figure 7 shows absorption and fluorescence spectra of the sulforhodamine B-doped film. Absorption and fluorescence peak tops were clearly observed at 565 and 585 nm, respectively. On the contrary, only a trace of sulforhodamine B was observed in the UV spectrum for a template-free TiO_2 film which underwent the same procedures (irradiation, immersion, and rinsing). It is clear that a sulforhodamine B molecule was incorporated into the nanocavity of the photoirradiated ABA/TiO_2 film. Slight red shifts of these spectral maxima relative to those of free sulforhodamine B molecules in methanol are explained by the difference in the microenvironment around the dye molecule. The amount of the embedded dye molecules was roughly calculated as 4% against the original amount of ABA by using UV spectroscopic results. It is clear that accommodation of sulforhodamine B molecules into the cavity is more difficult than that in the case of ABA accommodation. The larger size of the sulforhodamine B molecules may suppress their diffusion into the cavities. We attempted to obtain further information on the inner environment of the nanocavity (polarity, size, etc.) by using sodium 1-pyrenesulfonate as a molecular probe. Although incorporation of 1-pyrenesufonate into the nanocavity was confirmed by UV spectroscopy, any fluorescence could not be detected probably due to the fluorescence quenching by the TiO_2 matrix.

Subsequently, the regiospecific incorporation of sulforhodamine B was achieved as an example of fabrication of 2-D patterns based on a nanocavity. Selective UV irradiation was conducted by using a TEM grid (400 mesh) as photomask. Doping of sulforhodamine B was performed under the same conditions as mentioned above. Figure 8 shows a fluorescence microscopic image of the 2-D segmented nanocomposite film. Emission from sulforhodamine B was observed only in the photoirradiated area. Although weak emission was detected from the nonirradiated area (it may be attributed to surface-attached sulforhodamine B molecules), a high contrast was obtained between emissions from the irradiated and nonirradiated areas (over 100 times) as confirmed by the intensity profile, and high spatioresolution (50 μm) was obtained without any optimization of the experimental condition (irradiation time, immersion time, etc.).

Implications and Prospects

A 2-D segmented nanocomposite material was prepared by fabrication of a segmented nanocavity film upon selective

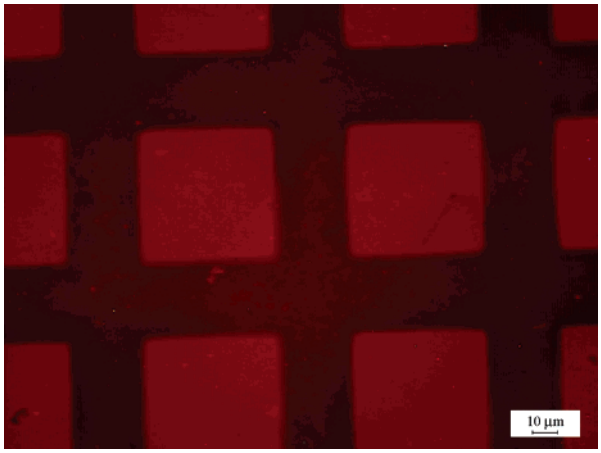

Figure 8. Fluorescence microscopic image of a 2-D patterned nanocomposite film.

photofabrication, followed by doping the cavity with organic molecule. An ABA molecule which is incorporated into the TiO_2 matrix generates N_2 gas by photoirradiation, and it creates a nanospace that can accommodate a small organic molecule. A simple example of a sequentially segmented nanocomposite material was demonstrated by photoirradiation of the ABA/TiO_2 film through a TEM grid as a photomask and subsequent doping of sulforhodamine B. The fluorescence microscopic image clearly indicates successful addressing of the sulforhodamine B molecule only on the irradiated area. Our approach on the fabrication of the 2-D segmented nanocomposite material was thus shown to be a useful methodology.

Although we could successfully prove the usefulness of the concept, further improvements are indispensable. The presence of the photoproduct within the nanocavity is a serious problem to be solved. It is strongly desired to develop a means to remove the photoproducts completely. In the present study, removal of the photoproduct by ethanol treatment led to simultaneous removal of unreacted ABA molecules because the photoproduct and ABA have similar solubilities. The use of a novel photoactive agent which undergoes drastic changes in the molecular property may solve this problem. As a second approach, photochemical detachment of a covalently linked photoactive agent would also solve the problem. A third possible improvement is the development of completely fragmented guest molecules upon photoirradiation.

Dye-doping into mesoporous structures (e.g., mesoporous silica, activated carbon fibers) is a useful method to fabricate nanocomposite materials. Many of their applications such as laser materials, solid-state sensors, and waveguide devices have already been demonstrated.[30−33] In the present paper, we showed addressing of the doped dye molecule with 2-D positional selectivity. This result would find many novel applications for nanocomposite materials. Photochemical patterning using a photomask and laser imaging enables to novel nanocomposite materials to be created with designed composite morphology. As further prospects, repetition of selective photoirradiation and doping will lead to fabrication of multiple nanocomposite materials in which a large variety of functional molecules are disposed on given segments. Even the creation of 3-D segmented nanocomposite materials can be envisaged by combination of the current concept with sensitizing dyes for two-photon absorption. The photofabrication of spatially segmented nanoporous structures may open a new area of research.

Supporting Information Available: Description of the calculation of the total adsorbed mass and the surface-adsorbed mass of ABA (PDF). This material is available free of charge via the Internet at http://pubs.acs.org.

CM050191A

(30) Telbiz, G.; Shvets, O.; Boron, S.; Vozny, V.; Brodyn, M.; Stucky, G. D. *Stud. Surf. Sci. Catal.* **2001**, *135*, 3564.
(31) Loerke, J.; Marlow, F. *Adv. Mater*. **2002**, *14*, 1745.
(32) Wark, M.; Rohlfing, Y.; Altindag, Y.; Wellmann, H. *Phys. Chem. Chem. Phys*. **2003**, *5*, 5188.
(33) Wirnsberger, G.; Scott, B. J.; Stucky, G. D. *Chem. Commun.* **2001**, *1*, 119.